

# Tokenizing Buildings: A Transformer for Layout Synthesis

Manuel Ladron de Guevara<sup>1</sup>, Jinmo Rhee<sup>2</sup>, Ardavan Bidgoli<sup>1</sup>, Vaidas Razgaitis<sup>1</sup>, and Michael Bergin<sup>1</sup>

<sup>1</sup> Higharc

manuelrodriguez@higharc.com, ardavanbidgoli@higharc.com,  
vaidasrazgaitis@higharc.com, michaelbergin@higharc.com

<sup>2</sup> University of Calgary, Canada

jinmo.rhee@ucalgary.ca

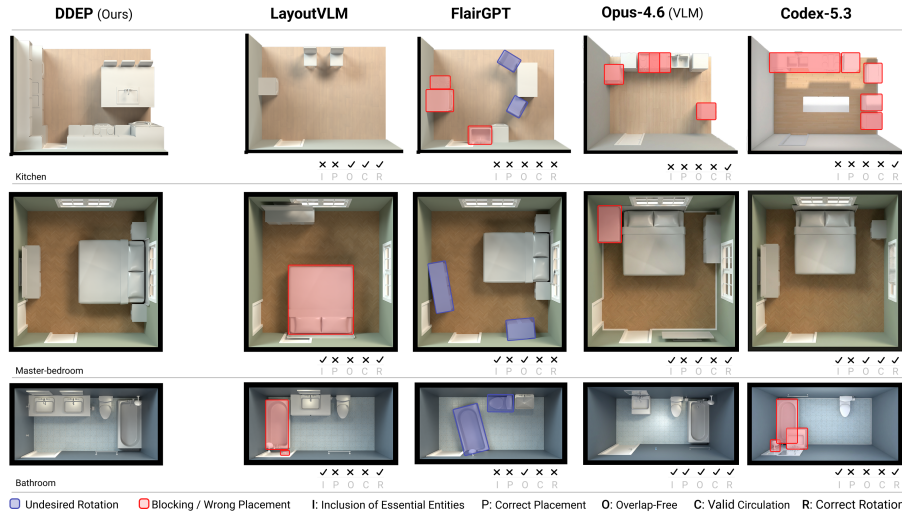


**Fig. 1:** Small Building Model (SBM) is an encoder-decoder Transformer that generates functionally correct and semantically coherent layouts given a room envelope. Each row shows a different room type. Our approach outperforms general-purpose LLMs/VLMs and domain-specific methods.

**Abstract.** We introduce Small Building Model (SBM), a Transformer-based architecture for layout synthesis in Building Information Modeling (BIM) scenes. We address the question of how to tokenize buildings by unifying heterogeneous feature sets of architectural elements into sequences while preserving compositional structure. Such feature sets are represented as a sparse attribute-feature matrix that captures room properties. We then design a unified embedding module that learns joint representations of categorical and possibly correlated continuous feature groups. Lastly, we train a single Transformer backbone in two modes: an encoder-only pathway that yields high-fidelity room embeddings, and an encoder-decoder pipeline for autoregressive prediction of residential room entities—referred to as Data-Driven Entity Prediction (DDEP).

Experiments across retrieval and generative layout synthesis show that SBM learns compact room embeddings that reliably cluster by type and topology, enabling strong semantic retrieval. In DDEP mode, SBM produces functionally sound layouts—with fewer collisions and boundary violations, and improved navigability—outperforming general-purpose LLM/VLM baselines and recent domain-specific methods. A controlled same-data benchmark confirms that these gains are architectural, not solely data-driven. An anonymized version of our dataset and code will be released upon acceptance.

## 1 Introduction

Professional Computer Aided Design (CAD)/BIM scenes encode rich semantics, hierarchies, and domain constraints, but most strong 3D generators—voxel, mesh, point-cloud, or image-conditioned diffusion models—treat scenes as unstructured geometry [3], yielding visually plausible yet hard-to-edit outputs that frequently violate basic validity rules. Room-scale layout design further demands multi-scale reasoning and parametric outputs compatible with downstream BIM tools, reflecting the highly constrained yet repetitive nature of practice, where designers position walls, doors, casework, and circulation to satisfy codes and programs across hundreds of similar rooms [1, 2, 4, 6]. Decades of computational approaches—from CAD macros and parametric families to rule systems, optimization, and learning-based methods—have aimed to automate this process [17], but progress remains bottlenecked not by algorithms themselves but by the representations they operate on. An effective representation must expose structure, generalize across typologies, and maintain BIM-level geometric and semantic coherence, underscoring the need to rethink spatial data encoding as the foundation for scalable layout reasoning.

To this end, we introduce a normalized hierarchical tokenizer that encodes room topology, entity attributes, wall-referenced geometry, and relational structure into compact *BIM-Token Bundles*. We realize these bundles as rows of a sparse attribute–feature matrix and embedded via a mixed-type module that produces a unified token vector for Transformer models. Building on this representation, our *SBM* provides a Transformer backbone for BIM scenes, supporting both encoder-only understanding of room embeddings at scale and encoder–decoder generation through *DDEP*, which autoregressively places room-level entities with mixed categorical and continuous attributes while preserving the compositional structure of BIM data.

In summary, we contribute (1) a normalized hierarchical tokenization of residential BIM scenes with a mixed-type embedding module, (2) a unified Transformer backbone (*SBM*) that supports both retrieval and generative layout synthesis through encoder-only and encoder–decoder (*DDEP*) modes, and (3) a two-track evaluation—a frontier LLM benchmark and a controlled same-data benchmark with ablations—demonstrating that *DDEP*’s advantages in scene coherence, geometric validity, and constraint satisfaction are architectural, not solely data-driven.

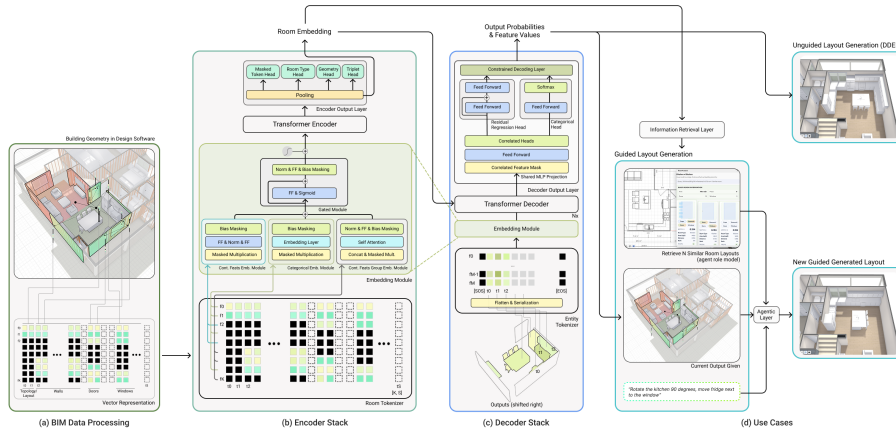


**Fig. 2:** Model overview. (a) BIM data extraction and assembly into a discrete set of token bundles. (b) SBM encoder stack processes the tokenized feature-attribute matrix and outputs a room representation. (c) SBM decoder stack consumes the room representation as memory to the cross-attention layers and the room entities as inputs, trained on next token prediction. (d) Use cases: our SBM is used for three main tasks: DDEP, information retrieval, and user-guided DDEP with the help of an agentic layer.

## 2 Related Work

*Rule-based and heuristic scene and layout generation.* Early work on automatic furniture layout relied on explicit design rules and expert heuristics encoded as constraints. Merrell et al. [16] incorporated interior design guidelines into a cost function and generated layout suggestions by sampling from it. Similarly, Song et al. [23] divided layouts into a few usage modes and applied mode-specific optimization strategies such as recursive subdivision and floor-field methods. Beyond these deterministic rule systems, some approaches convert design guidelines into objective terms and use search-based optimization—such as genetic algorithms—to explore a wider solution space while still operating on the same rule set [10].

*Deep learning-based scene and layout generation.* Graph-based generative models represent layouts as scene graphs and synthesize object arrangements by predicting node attributes and relational edges [7, 31]. Image- and feature-based neural models—ranging from GANs and transformers [15, 27] to hybrid vectorized systems like HouseDiffusion [22]—learn strong statistical priors for furniture placement yet still depend heavily on training distributions and often require post-hoc refinement to satisfy geometric and functional constraints. Diffusion-based models further improve controllability and semantic consistency, via conditional GAN refinement [18], mixed discrete-continuous diffusion for 3D scenes [8], room-mask-conditioned semantic diffusion [26], multi-view RGB-D generation [19], and text-to-layout diffusion Transformers [21, 24].

*Transformer-based indoor-scene synthesis (object-centric).* A closely related line of work treats *indoor scene synthesis* as Transformer-driven generation of object instances (category and pose) conditioned on a room boundary or floor-plan mask. ATISS [20] and SceneFormer [29] generate sequences (or sets) of furniture objects with discretized/normalized geometric attributes, targeting visually plausible and collision-free arrangements in synthetic scene datasets. CLIP-Layout [14] further augments this object-centric paradigm with semantic furniture embeddings (via CLIP) to encourage style consistency and improve instance-level retrieval during generation. While highly relevant, these approaches largely assume a *flat* object vocabulary (furniture instances with poses) and do not model the heterogeneous, hierarchical, and parametric nature of BIM: envelopes and walls, wall-hosted elements, typed constraints, and mixed categorical–continuous attributes that must remain editable in downstream CAD/BIM workflows. This mismatch motivates BIM-native tokenization and embedding that preserve compositional structure (e.g., envelope  $\rightarrow$  boundaries  $\rightarrow$  hosted entities) and enable constraint-aware reasoning beyond object boxes.

In parallel, controllable *2D* layout generation for graphic design has been studied with Transformer formulations such as BLT [9], which uses bidirectional/masked prediction and iterative refinement to satisfy user constraints while accelerating inference.

*LLM/VLM-based scene and layout generation.* Language-based models have recently been applied to spatial layout generation by representing scenes as token sequences. LayoutGPT [5] frames layout synthesis as compositional planning, generating object–relation tokens autoregressively, though it remains reliant on prompting and lacks continuous geometric grounding. Vision-language approaches such as LayoutVLM [25] embed spatial cues jointly with textual descriptions to optimize 3D layouts, yet their coupling of vision features and natural language does not yield a normalized geometric token space.

Other systems use LLMs for guided refinement: HouseTune [33] proposes and linguistically adjusts floorplan candidates, while FlairGPT [13] aligns language tokens with furniture and style attributes for interior design exploration. Multi-modal models like LLM4CAD [11] tokenize CAD elements symbolically to support reasoning but operate at the object level without encoding continuous spatial attributes or wall-referenced coordinates. Recently, FloorPlan-DeepSeek [32] formulates floorplan synthesis as autoregressive next-room prediction, encoding each room as a vector of semantic type and geometric attributes. This sequential approach constructs layouts incrementally from partial plans or text prompts, achieving improved structural coherence and enabling downstream editing. However, the approach remains limited to room-level floor-plan arrangement, and does not encode fine-grained BIM elements or wall-hosted entities. Across this progression, existing representations still fail to unify semantic, relational, and geometric information in a sequence-native form with mixed categorical–continuous attributes, limiting constraint-aware reasoning and downstream BIM editability. This gap motivates our normalized BIM tokenization coupled with a shared Transformer backbone.

### 3 Method

#### 3.1 Problem Setup and BIM Room Representation

We operate on residential room-level layouts extracted from professional BIM projects (see Sec. 4 for dataset details), expressed in a local coordinate frame normalized for position and scale.

*Envelope vs. contents.* Each room is decomposed into a *room envelope*—walls, openings, and coarse layout attributes—and *room contents* (props and casework):  $r_{\text{env}} = (y^{\text{topo}}, y^{\text{layout}}, \mathcal{E}, \mathcal{D}, \mathcal{W})$ ,  $r_{\text{ent}} = (\mathcal{P}, \mathcal{C})$  and define the full room as  $r = (r_{\text{env}}, r_{\text{ent}})$ . Here  $y^{\text{topo}}$  is a discrete room-type token (e.g., *bedroom*, *kitchen*) and  $y^{\text{layout}}$  is a layout token that aggregates global scalar attributes such as area and perimeter. The sets  $\mathcal{E}, \mathcal{D}, \mathcal{W}$  are walls, doors, and windows, and  $\mathcal{P}, \mathcal{C}$  are props and casework, respectively. In our model, the *encoder* operates only on the envelope  $r_{\text{env}}$ , while the *decoder* operates only on the entity sequence  $r_{\text{ent}}$  conditioned on the encoder output.

*Walls and room topology.* The room boundary and internal partitions are represented as a set of  $N_E$  directed wall segments  $\mathcal{E} = \{e_j\}_{j=1}^{N_E}$ ,  $e_j = (x_j^{(1)}, x_j^{(2)}, a_j^{\text{wall}})$ , where  $x_j^{(1)}, x_j^{(2)} \in \mathbb{R}^2$  are the endpoints in the local coordinate frame and  $a_j^{\text{wall}}$  collects wall attributes (e.g., inside/outside thickness, wall condition or construction type, and a discrete edge identifier). The counter-clockwise ordered set  $\mathcal{E}$  defines the room polygon and its topology; global geometric scalars such as area and perimeter are computed from  $\mathcal{E}$  and packed into the layout token  $y^{\text{layout}}$ .

*Openings: doors and windows.* Doors and windows are modeled as objects attached to specific wall edges with wall-referenced coordinates. For doors we write  $\mathcal{D} = \{d_k\}_{k=1}^{N_D}$ ,  $d_k = (j_k, t_k, w_k, a_k^{\text{door}})$ , where  $j_k \in \{1, \dots, N_E\}$  indexes the supporting edge  $e_{j_k}$ ,  $t_k \in [0, 1]$  is a normalized position along that edge,  $w_k$  is the opening width, and  $a_k^{\text{door}}$  includes additional categorical attributes (e.g., door family/type, swing direction). Windows  $\mathcal{W} = \{w_\ell\}_{\ell=1}^{N_W}$  are defined analogously. This wall-referenced parameterization makes openings invariant to absolute translation and scale.

*Furniture and casework entities.* Room contents are represented as two sets of entities:  $\mathcal{P} = \{p_u\}_{u=1}^{N_P}$ ,  $\mathcal{C} = \{c_v\}_{v=1}^{N_C}$ , for props (furniture) and casework. Each entity is parameterized by a discrete type and a small set of wall-referenced continuous attributes. For a generic entity  $q \in \mathcal{P} \cup \mathcal{C}$  we write  $q = (c_q, j_q, t_q, \delta_q, s_q, \rho_q, a_q^{\text{ent}})$ , where  $c_q$  is an entity type identifier (e.g., *bed*, *base\_cabinet*),  $j_q$  is the supporting edge index,  $t_q \in [0, 1]$  is the position along that edge,  $\delta_q$  is a signed lateral offset from the wall,  $s_q$  encodes size parameters (e.g., width/depth),  $\rho_q$  is an in-plane rotation (props only), and  $a_q^{\text{ent}}$  contains additional categorical attributes.

*Tasks.* Given this decomposition, our model supports two tasks. In *encoder-only* mode, the goal is to map the room envelope  $r_{\text{env}}$  to a compact embedding  $z(r_{\text{env}}) \in \mathbb{R}^d$  that preserves semantic and geometric relationships between rooms

(for retrieval and analysis). In *encoder–decoder* mode (DDEP), the encoder consumes only the envelope  $r_{\text{env}}$  to produce a contextual memory, and the decoder autoregressively generates the entity sequence  $r_{\text{ent}} = (\mathcal{P}, \mathcal{C})$  as a sequence of tokens (see Fig. 2).

### 3.2 BIM Tokenization

Given the room envelope  $r_{\text{env}}$  and contents  $r_{\text{ent}}$  (Sec. 3.1), we convert each room into two ordered sequences of *BIM-Token Bundles*: an envelope sequence for the encoder and an entity sequence for the decoder. Each bundle corresponds to a single logical element (topology, layout, wall, door, window, or entity) and aggregates all of its semantic and geometric attributes into a sparse feature vector.

*Token sequences.* On the encoder side, we construct a fixed-order sequence that starts with a special classification token and ends with an end-of-sequence token:

$$(\tau^{\text{CLS}}, \tau^{\text{t}}, \tau^{\text{l}}, \tau_1^{\text{e}}, \dots, \tau_{N_E}^{\text{e}}, \tau_1^{\text{d}}, \dots, \tau_{N_D}^{\text{d}}, \tau_1^{\text{w}}, \dots, \tau_{N_W}^{\text{w}}, \tau^{\text{EOS}}),$$

followed by padding tokens up to a maximum length  $S_{\text{enc}}$ . The CLS bundle  $\tau^{\text{CLS}}$  is a learnable summary token used for pooling in encoder-only mode; it does not correspond to any specific BIM element. The topology bundle  $\tau^{\text{t}}$  encodes  $y^{\text{topo}}$  (room type), the layout bundle  $\tau^{\text{l}}$  encodes  $y^{\text{layout}}$  (area, perimeter, and other global scalars), each edge bundle  $\tau_j^{\text{e}}$  aggregates the attributes of  $e_j \in \mathcal{E}$ , and each door or window bundle aggregates the corresponding element in  $\mathcal{D}$  or  $\mathcal{W}$  with wall-referenced parameters. The EOS bundle  $\tau^{\text{EOS}}$  marks the end of the envelope sequence. This encoder sequence is *envelope-only*: props and casework are not encoded in the encoder input.

On the decoder, we form a content only entity sequence  $(\tau^{\text{SOS}}, \tau_1^{\text{ent}}, \dots, \tau_T^{\text{ent}}, \tau^{\text{EOS}})$ , where each  $\tau_t^{\text{ent}}$  corresponds to one entity  $q \in \mathcal{P} \cup \mathcal{C}$  with its type and wall-referenced attributes, and  $\tau^{\text{SOS}}, \tau^{\text{EOS}}$  are special start/end tokens. The room envelope is provided to the decoder only via cross-attention to the encoder memory, not re-encoded as decoder tokens.

*Attribute–feature matrices.* We realize these heterogeneous token sequences as *attribute–feature matrices* with a fixed feature axis and variable sequence length. For the encoder, we define  $X^{\text{enc}} \in \mathbb{R}^{F_{\text{enc}} \times S_{\text{enc}}}$ ,

$$X^{\text{enc}} = \begin{bmatrix} x_{1,1}^{\text{enc}} & x_{1,2}^{\text{enc}} & \cdots & x_{1,S_{\text{enc}}}^{\text{enc}} \\ x_{2,1}^{\text{enc}} & x_{2,2}^{\text{enc}} & \cdots & x_{2,S_{\text{enc}}}^{\text{enc}} \\ \vdots & \vdots & \ddots & \vdots \\ x_{F_{\text{enc}},1}^{\text{enc}} & x_{F_{\text{enc}},2}^{\text{enc}} & \cdots & x_{F_{\text{enc}},S_{\text{enc}}}^{\text{enc}} \end{bmatrix},$$

where each *column*  $X_{:,s}^{\text{enc}}$  encodes one BIM-Token Bundle at sequence position  $s$ , and each *row* corresponds to a specific feature. The first rows are two generic categorical identifiers that are present for every token, a *type id* to denote the semantic attribute, and a *token id* to index each semantic instance within each

type. The remaining rows collect room-level scalars (e.g., area, perimeter), wall geometry (edge endpoints, lengths, thicknesses), and opening parameters (normalized position along the wall, width, corner distances), as configured in a fixed feature table. Only a subset of these features is active for any given token type; non-applicable entries are filled with a designated padding value, yielding a sparse representation. A complete list of encoder feature rows is provided in the supplement.

We construct the decoder matrix  $X^{\text{dec}} \in \mathbb{R}^{F_{\text{dec}} \times S_{\text{dec}}}$  in the same way, now with decoder-specific features such as entity type, edge attachment, wall-referenced coordinates  $(t_q, \delta_q)$ , size parameters  $s_q$ , and rotation  $\rho_q$ , plus *token type id* and *token id*. Here too, only the rows relevant to each token type are active and the rest are set to  $p = -100$ .

### 3.3 Mixed-Type Embedding Module

The BIM-Token Bundles defined above combine heterogeneous categorical and continuous attributes on a shared feature axis. Our mixed-type embedding module converts the sparse feature matrices  $X^{\text{enc}}$  and  $X^{\text{dec}}$  into dense token embeddings suitable for a Transformer, while respecting which features are active for which tokens.

Formally, we define two embedding maps

$$\Phi_{\text{enc}} : \mathbb{R}^{F_{\text{enc}} \times S_{\text{enc}}} \rightarrow \mathbb{R}^{S_{\text{enc}} \times d}, \quad \Phi_{\text{dec}} : \mathbb{R}^{F_{\text{dec}} \times S_{\text{dec}}} \rightarrow \mathbb{R}^{S_{\text{dec}} \times d},$$

implemented by a shared *FeatureEmbedding* module configured with encoder- or decoder-specific feature definitions. In both cases, each token embedding is constructed by summing the contributions of all its active features.

*Feature-wise embeddings and masking.* Consider first the encoder. For a single room, the encoder feature matrix  $X^{\text{enc}}$  has rows  $x_f \in \mathbb{R}^{S_{\text{enc}}}$  corresponding to individual features (e.g., *token\_type\_id*, *area*, *edge\_x1*, *t\_value*). For each feature  $f$  we instantiate a feature-specific embedding function  $E_f$ :

- **Categorical features** (e.g., *token\_type\_id*, *token\_id*, edge indices, wall condition) use learnable embedding tables  $E_f : \mathbb{Z} \rightarrow \mathbb{R}^d$  with a dedicated entry for padding.
- **Scalar continuous features** (e.g., area, perimeter, edge length, relative length) use small multilayer perceptrons  $E_f : \mathbb{R} \rightarrow \mathbb{R}^d$ .
- **Grouped continuous features** (e.g., edge endpoint coordinates, thickness pairs, door/window corner distances) use a *MultiContinuousEmbedding*: a lightweight sub-network that embeds each scalar in the group, applies self-attention or pooling across the group, and projects the result to  $\mathbb{R}^d$ .

Let  $\mathcal{F}_{\text{enc}}$  be the set of encoder features. For each feature  $f \in \mathcal{F}_{\text{enc}}$  and token position  $s$ , we define a valid-feature mask  $m_{f,s} = \mathbb{1}[X_{f,s}^{\text{enc}} \neq -100]$ , which indicates whether feature  $f$  applies to token  $s$ . We then compute feature embeddings and apply the mask:  $u_{f,s} = E_f(X_{f,s}^{\text{enc}}) \in \mathbb{R}^d$ ,  $\tilde{u}_{f,s} = m_{f,s} \cdot u_{f,s}$ . This second masking step ensures that inactive features contribute exactly zero, including the bias terms of linear layers.

*Token embedding as feature sum.* The final encoder token embedding at position  $s$  is the sum of all active feature embeddings for that token:  $e_s^{\text{enc}} = \sum_{f \in \mathcal{F}_{\text{enc}}} \tilde{u}_{f,s} \in \mathbb{R}^d$ . Stacking these over sequence positions yields  $E^{\text{enc}} = \Phi_{\text{enc}}(X^{\text{enc}}) \in \mathbb{R}^{S_{\text{enc}} \times d}$ , optionally augmented with learned positional embeddings. This construction is token-type agnostic: topology, layout, walls, doors, and windows are all embedded via the same mechanism, differing only in which feature rows are active for each token.

*Decoder embeddings.* The decoder uses the same FeatureEmbedding architecture with a decoder-specific feature set. Given the decoder feature matrix  $X^{\text{dec}}$ , we instantiate analogous categorical, continuous, and grouped-continuous embedders for features such as *token\_type\_id*, *token\_id*, edge attachments, wall-referenced coordinates  $(t_q, \delta_q)$ , size parameters  $s_q$ , and rotations  $\rho_q$ . Applying the same masking and summation procedure yields decoder token embeddings  $E^{\text{dec}} = \Phi_{\text{dec}}(X^{\text{dec}}) \in \mathbb{R}^{S_{\text{dec}} \times d}$ , with the property that entities of different types (props vs. casework, SOS/EOS vs. regular tokens) share the same embedding space but rely on different subsets of features.

### 3.4 Transformer Backbone and Operating Modes

Given the token embeddings we employ a standard Transformer encoder–decoder architecture. The same backbone is used in two operating modes: encoder-only (for room embeddings and retrieval) and encoder–decoder (for data-driven entity prediction, DDEP).

*Encoder-only: room embeddings and retrieval.* In encoder-only mode, we use only the Transformer encoder. Given  $E^{\text{enc}}$  and an attention mask over non-padding tokens, we compute  $M = \text{Enc}_{\theta}(E^{\text{enc}}) \in \mathbb{R}^{S_{\text{enc}} \times d}$ , where  $\text{Enc}_{\theta}$  is a stack of self-attention and feed-forward blocks. The first position in the sequence corresponds to the special CLS token  $\tau^{\text{CLS}}$  introduced in Sec. 3.2. We obtain a room embedding for the envelope by pooling at this position  $z(r_{\text{env}}) = M_0 \in \mathbb{R}^d$ , which we use directly for room retrieval and similarity-based analysis. Encoder heads (e.g., room-type classification and masked-token prediction) operate on  $z(r_{\text{env}})$  and on the full memory  $M$ .

*Encoder–decoder: Data-Driven Entity Prediction (DDEP).* In DDEP mode, we use the full encoder–decoder Transformer to generate the room contents  $r_{\text{ent}} = (\mathcal{P}, \mathcal{C})$  conditioned on the room envelope  $r_{\text{env}}$ . The encoder processes the envelope as above, producing a memory  $M$  that is held fixed during decoding. The decoder takes entity token embeddings  $E^{\text{dec}}$  and attends both to the prefix of generated tokens (causal self-attention) and to the encoder memory  $M$  (cross-attention),  $H = \text{Dec}_{\theta}(E^{\text{dec}}, M) \in \mathbb{R}^{S_{\text{dec}} \times d}$ , where  $\text{Dec}_{\theta}$  is a stack of masked self-attention, cross-attention, and feed-forward layers. Decoder states in  $H$  feed into multi-head prediction layers that produce mixed categorical and continuous outputs for each entity token. At inference time, a constrained decoding layer enforces BIM validity constraints (e.g., egress clearances, door-swing zones) by filtering the model’s output distribution at each step, ensuring structurally valid token sequences without external guidance (details in Suppl.).

*Training.* We adopt a two-stage schedule. First, the encoder is pre-trained on the full corpus with a composite loss combining room-type classification, masked-token modeling, graded triplet contrastive learning, and geometric preservation. Second, the encoder-decoder model is fine-tuned for DDEP using teacher forcing: at each step the decoder predicts the next entity token given the ground-truth prefix, with a combined cross-entropy loss over categorical heads and MSE loss over continuous regression heads. Full loss formulations, hyperparameters, and infrastructure details are provided in the Supplementary Material.

## 4 Experiments and Results

We evaluate DDEP and SBM embeddings on a proprietary corpus of residential BIM scenes (single-family homes with typed rooms). Training, implementation details, and full tokenizer/adaptor configurations are in the Supplementary Material. We report DDEP results under two complementary protocols whose rows are not directly comparable.

**Frontier LLM Benchmark.** Production DDEP is trained per room type on the full augmented corpus (439,932 samples) and compared to frontier LLMs, VLMs, and domain-specific baselines under deployment-realistic conditions on a 50-room held-out set.

**Controlled Same-Data Benchmark.** A frozen split of 15,740/2,009/1,826 (train/val/test) rooms across five types (`bathfull`, `bedroom`, `laundry`, `living`, `master_bed`) with shared ontology normalization, adapters, and evaluation harness for all methods. The camera-ready metric pipeline first filters this test split to the 1,231-room geometry-valid subset, and Table 2 reports the shared 1,225-room intersection on which all compared methods materialize outputs under this harness. This protocol isolates architectural differences under matched data conditions.

*Metrics.* We report three complementary metrics, all computed with identical room geometry, entity dimensions, and inventory specifications across methods. **Coverage** ( $\uparrow$ ) measures inventory satisfaction: the weighted fraction of required items and alternative groups fulfilled, penalizing extraneous categories. **Navigability** ( $\uparrow$ ) evaluates functional access via A\*-based pathfinding from inward-offset door portals to essential targets. Doorways must remain valid entry points: if the portal or immediate inward vestibule is blocked, that door contributes failed door-target pairs except for a tiny raster snap used only for numerical robustness. For reachable pairs we compare shortest-path length  $\ell_t$  to straight-line distance  $\ell_t^*$  through a capped detour penalty, and report  $\text{Nav} = 100 \times (\text{SR} - \lambda \text{DF})$  with  $\lambda = 0.35$ . When nothing is reachable, DF defaults to its worst value and Nav reaches its minimum of  $-35$ . **Overlap & Clearance** (OC,  $\downarrow$ ) reports the weighted composite of entity overlap fraction, global overlap area, and door-clearance intrusion; wall-bounds violation is tracked separately in the Supplement. Full definitions, including Coverage formulation and OC weights, are in the Supplement.

**Table 1: Frontier LLM Benchmark.** Comparison of frontier LLMs on the 50-room held-out set. We report mean  $\pm$  std. Higher is better for Coverage and Navigability (mean and SR); lower is better for OC, DF, and latency. OC reports the weighted overlap-clearance composite defined in the Supplement. Best text/VLM method per metric in **bold** among those evaluated on all 50 rooms; subset-evaluated models are excluded from bolding. All methods use the same unguided prompt with entity catalog (information parity.) <sup>†</sup>Evaluated on a subset of rooms due to low parse success rate ( $<70\%$ ). <sup>‡</sup>Evaluated on 37/50 rooms. <sup>§</sup>Evaluated on 7/50 rooms (unreliable). LayoutVLM requires an initial furniture list as input, so it is excluded from Coverage.

Method	Coverage		Navigability		OC (%)	Inference Latency (s)
	$\uparrow$ mean $\pm$ std	$\uparrow$ mean $\pm$ std	$\uparrow$ SR (mean $\pm$ std)	$\downarrow$ DF (mean $\pm$ std)	$\downarrow$ mean $\pm$ std	$\downarrow$ mean $\pm$ std
<i>Text-based methods</i>						
Claude Opus 4.6	58.9 $\pm$ 37.0	-0.8 $\pm$ 56.3	0.26 $\pm$ 0.43	0.75 $\pm$ 0.40	11.3 $\pm$ 11.1	15.6
GPT-5.2 <sup>†</sup>	47.6 $\pm$ 36.3	16.8 $\pm$ 54.7	0.35 $\pm$ 0.40	0.53 $\pm$ 0.47	13.0 $\pm$ 13.5	55.1
Claude Sonnet 4.6	64.9 $\pm$ 35.9	0.3 $\pm$ 53.3	0.25 $\pm$ 0.39	0.70 $\pm$ 0.43	10.5 $\pm$ 11.5	81.2
Gemini 3.1 Pro <sup>‡</sup>	63.7 $\pm$ 37.2	20.5 $\pm$ 60.7	0.40 $\pm$ 0.46	0.56 $\pm$ 0.46	9.2 $\pm$ 14.0	67.1
<b>Codex 5.3</b>	<b>68.3 <math>\pm</math> 34.2</b>	<b>18.9 <math>\pm</math> 55.8</b>	<b>0.37 <math>\pm</math> 0.42</b>	<b>0.52 <math>\pm</math> 0.46</b>	<b>9.8 <math>\pm</math> 11.4</b>	20.8
Claude Haiku 4.5	55.3 $\pm$ 38.3	4.4 $\pm$ 56.7	0.28 $\pm$ 0.43	0.69 $\pm$ 0.43	15.2 $\pm$ 14.5	7.0
Qwen 3.5	64.6 $\pm$ 31.5	3.1 $\pm$ 51.7	0.26 $\pm$ 0.37	0.66 $\pm$ 0.44	13.6 $\pm$ 15.5	19.0
<i>VLM methods</i>						
Claude Opus 4.6	61.9 $\pm$ 36.7	<b>55.5 <math>\pm</math> 56.1</b>	<b>0.66 <math>\pm</math> 0.44</b>	<b>0.29 <math>\pm</math> 0.40</b>	<b>8.2 <math>\pm</math> 11.7</b>	15.3
GPT-5.2 <sup>†</sup>	57.0 $\pm$ 38.3	34.9 $\pm$ 60.3	0.51 $\pm$ 0.46	0.46 $\pm$ 0.47	12.1 $\pm$ 11.8	101.7
<b>Claude Sonnet 4.6</b>	<b>65.6 <math>\pm</math> 35.3</b>	34.6 $\pm$ 58.7	0.50 $\pm$ 0.45	0.43 $\pm$ 0.44	11.0 $\pm$ 13.2	14.8
Gemini 3.1 Pro <sup>§</sup>	86.5 $\pm$ 12.6	47.8 $\pm$ 65.3	0.61 $\pm$ 0.49	0.38 $\pm$ 0.48	2.2 $\pm$ 3.0	-
Claude Haiku 4.5	60.7 $\pm$ 36.1	25.2 $\pm$ 59.6	0.42 $\pm$ 0.46	0.49 $\pm$ 0.46	16.2 $\pm$ 15.7	6.9
Qwen 3.5 <sup>†</sup>	60.7 $\pm$ 36.5	27.1 $\pm$ 54.8	0.42 $\pm$ 0.41	0.42 $\pm$ 0.46	12.8 $\pm$ 15.9	84.1
<i>Domain-specific methods</i>						
LayoutVLM	-	40.3 $\pm$ 59.8	0.55 $\pm$ 0.45	0.41 $\pm$ 0.45	3.8 $\pm$ 7.3	144.99 $\pm$ 36.50
FlairGPT	46.6 $\pm$ 36.5	28.2 $\pm$ 61.0	0.46 $\pm$ 0.46	0.51 $\pm$ 0.46	3.9 $\pm$ 8.1	1133.61 $\pm$ 1596.40
<b>DDEP (Ours)</b>	<b>98.1 <math>\pm</math> 6.3</b>	<b>79.2 <math>\pm</math> 44.7</b>	<b>0.86 <math>\pm</math> 0.34</b>	<b>0.20 <math>\pm</math> 0.32</b>	<b>1.9 <math>\pm</math> 3.1</b>	<b>3.18 <math>\pm</math> 0.18</b>

## 4.1 Frontier LLM Benchmark

We compare production DDEP against frontier LLMs and VLMs (text-only and image-conditioned variants of Claude Opus/Sonnet 4.6, Claude Haiku 4.5, GPT-5.2, Gemini 3.1 Pro, Codex 5.3, and Qwen 3.5) and domain-specific baselines (LayoutVLM [25], FlairGPT [13]), all used off-the-shelf (inference only) with our room representation adapted to each method’s input format. All baselines receive the same unguided prompt with entity catalog; VLMs additionally condition on a 1024 $\times$ 1024 floorplan render. Free-text outputs are parsed via a rule-based mapper to our inventory (details in Suppl.). Because frontier API costs limit the test set to 50 rooms, this benchmark characterizes deployment-realistic performance across many baselines; the controlled same-data benchmark (Sec. 4.2) provides the larger-scale statistical analysis.

Table 1 shows that production DDEP achieves 98.1 coverage, 79.2 navigability, and 1.9% OC, outperforming all baselines on coverage, navigability, and composite overlap-clearance simultaneously. Under the stricter doorway-validity metric, frontier performance drops substantially: the strongest fully evaluated text model is Codex 5.3 with 68.3 coverage and 18.9 navigability, while the strongest fully evaluated VLM is Claude Opus 4.6 with 55.5 navigability and Claude Sonnet 4.6 with 65.6 coverage. Domain-specific baselines (FlairGPT, LayoutVLM) narrow the OC gap (3.9% and 3.8%, respectively) but remain sub-

**Table 2: Controlled Same-Data Benchmark.** Controlled benchmark on the frozen same-data split, reported on the shared 1,225-room intersection of successfully materialized outputs across all methods. All methods use canonical furniture dimensions and a shared denormalization pipeline with unified metrics computation. OC reports the weighted overlap-clearance composite defined in the Supplement. Inference latency is omitted in this controlled benchmark. Rows in this table are not directly comparable to Table 1 due to different training protocols. Nav can be negative because unreachable rooms receive the worst detour penalty under the doorway-validity definition (see Sec. 4).

Method	Coverage		Navigability		OC (%)
	↑ mean ± std	↑ mean ± std	↑ SR (mean ± std)	↓ DF (mean ± std)	↓ mean ± std
ATISS [20] (same-data)	40.8 ± 23.6	-30.3 ± 24.0	0.03 ± 0.18	0.97 ± 0.18	0.5 ± 2.5
BLT [9] (same-data)	17.8 ± 20.4	-18.6 ± 42.7	0.12 ± 0.32	0.88 ± 0.31	35.7 ± 16.9
<b>DDEP (Ours)</b>	<b>54.9 ± 38.3</b>	<b>14.6 ± 56.0</b>	<b>0.36 ± 0.42</b>	<b>0.60 ± 0.44</b>	<b>13.4 ± 12.5</b>
<i>DDEP ablations</i>					
Wall-Only	50.8 ± 39.6	9.6 ± 54.8	0.32 ± 0.41	0.63 ± 0.44	12.7 ± 11.8
No Continuous Groups	42.6 ± 40.2	0.7 ± 52.2	0.25 ± 0.39	0.69 ± 0.43	13.4 ± 13.8
No Edge Coordinates	56.7 ± 39.7	14.4 ± 57.6	0.35 ± 0.43	0.60 ± 0.45	14.5 ± 12.7
Order: t_value First	42.6 ± 39.1	4.1 ± 54.5	0.29 ± 0.41	0.70 ± 0.41	10.6 ± 12.0
Order: edge,t_value Desc	46.5 ± 39.9	7.8 ± 54.8	0.31 ± 0.41	0.66 ± 0.42	13.4 ± 13.2

stantially weaker on coverage and navigability, indicating that DDEP’s BIM-native tokenization and wall-referenced decoding jointly enable the strongest balance across all three axes.

## 4.2 Controlled Same-Data Benchmark

We compare DDEP against ATISS [20], BLT [9], and five DDEP ablations—eight models trained from scratch on the frozen controlled split under a uniform, resource-matched protocol: a fixed budget of 200 training epochs, shared ontology normalization, canonical furniture dimensions, and a common evaluation harness with no method-specific tuning.

*Baselines.* DDEP achieves 54.9 coverage and 14.6 navigability on the shared 1,225-room controlled subset (Table 2), outperforming ATISS by +14.1 coverage and +44.9 navigability and BLT by +37.1 coverage and +33.2 navigability. ATISS was designed for 3D-FRONT-style scenes with axis-aligned bounding boxes; we decode its outputs with its published descale formula, affine-map positions into the physical room, and project to the nearest wall edge to obtain wall-referenced coordinates (full pipeline in Suppl.). BLT targets 2D graphic-design layout; its  $(x, y, w, h)$  outputs are similarly projected. Both baselines use their published default hyperparameters with no method-specific tuning. The resulting bridge is shared between baselines, so it cannot explain DDEP’s advantage. ATISS’s near-zero OC (0.5%) should not be read as superior spatial validity: many ATISS outputs are sparse or nearly empty, which trivially avoids collisions but yields strongly negative navigability. BLT shows the complementary failure mode, with 35.7% OC and only 0.12 SR. DDEP is the only method that maintains nontrivial coverage, positive navigability, and moderate OC under the same-data protocol.



**Fig. 3:** Qualitative comparison of generated layouts across five room types, showing representative results from seven baseline methods and our DDEP model.

Controlled DDEP scores are lower than production DDEP (54.9 vs. 98.1 coverage) because the controlled protocol deliberately constrains every method to the same resource envelope:  $\sim 28\times$  less training data (15.7K vs. 439.9K rooms), a single 256-dim model serving five room types jointly (vs. per-type 512-dim specialists), and 200 training epochs. ATISS, BLT, and all five ablations operate under these same constraints. The gap between controlled and production DDEP quantifies the combined data-and-scale contribution, while the controlled benchmark isolates the architectural signal.

*Ablation analysis.* Five ablations probe key design choices (Table 2, bottom). We report deltas relative to the full DDEP model (54.9 coverage, 14.6 navigability). The ordering is stable across the shared 1,225-room subset: removing continuous-group embeddings is the most damaging change, while removing explicit edge coordinates is nearly neutral on coverage and navigability but still hurts overlap-clearance.

*No Continuous Groups* ( $-12.3$  cov,  $-13.9$  nav) replaces the multi-continuous embedding which jointly embeds correlated continuous features (e.g., edge coordinates, thickness pairs) via self-attention—with independent scalar MLPs. This is the most damaging single change, confirming that joint embedding of correlated geometric attributes is critical for spatial reasoning.

*Ordering ablations.* *t\_value First* ( $-12.3$  cov,  $-10.5$  nav) reorders entities by wall-referenced position before edge index; *edge,t\_value Desc* ( $-8.4$  cov,  $-6.8$  nav) reverses the within-wall sort direction. Both confirm that the canonical edge-then-position ordering provides an inductive bias the model relies on, with edge grouping mattering most.

**Table 3:** Embedding Quality Across Type-Constrained Retrieval, Clustering, and Geometric Correlation

Method	Type-Constrained Retrieval @ $k = 5$			Clustering & Geometric Correlation			
	nDCG	Triplet	Entity Sim	NMI	ARI	Silhouette	Spearman
SBM	68.2	99.9	77.0	<b>0.726</b>	<b>0.437</b>	<b>0.141</b>	0.184
E5-Large-v2	<b>86.7</b>	99.9	<b>78.4</b>	0.371	-0.019	0.051	<b>0.315</b>
BGE-Large-en-v1.5	80.1	99.9	77.0	0.358	-0.003	0.069	0.235
GTE-Large-en-v1.5	74.3	99.8	77.0	0.335	-0.002	0.067	0.133

*Wall-Only* ( $-4.1$  cov,  $-5.0$  nav) strips doors and windows from the encoder. The moderate drop confirms that opening positions help the decoder reason about clearances, though walls alone provide a useful baseline signal.

*No Edge Coordinates* ( $+1.8$  cov,  $-0.2$  nav) removes wall endpoint coordinates while retaining lengths, thicknesses, and opening parameters. The near-tie suggests the model infers relative geometry from remaining features; however, OC rises from 13.4% to 14.5%. Per-room-type breakdowns are in the Supplement.

Notably, the two largest ablation effects—joint continuous embedding and entity ordering—each cause double-digit coverage drops, indicating that these representation design choices, not model scale or architecture depth alone, are primary drivers of DDEP’s advantage.

### 4.3 Qualitative Comparisons

Figures 1 and 3 shows example layouts for several room types from DDEP, VLMs, and domain-specific methods. VLM baselines often overfill rooms with extra casework and furniture, blocking circulation and door clearances, especially in living rooms and garages. Domain-specific methods tend to place more appropriate furniture types but still leave narrow or blocked paths around key elements. In contrast, DDEP produces layouts that satisfy the room program while keeping clear, door-connected circulation bands and respecting wall-referenced anchoring, visually matching the trends reported in our quantitative metrics.

### 4.4 Embedding Evaluation and Encoder Ablations

We evaluate SBM’s encoder-only pathway for room embedding quality through retrieval and clustering benchmarks, comparing against three text embedding baselines: E5-Large-v2 [28] (560M params), BGE-Large-en-v1.5 [30] (335M), and GTE-Large-en-v1.5 [12] (335M). All three are pre-trained on web-scale corpora (orders of magnitude more data than SBM’s domain-specific dataset). For fair comparison, we serialize room data to text format so that text embeddings process the same room information.

*Evaluation Metrics* We assess type-constrained retrieval (nDCG@k, triplet accuracy, entity overlap), clustering quality (NMI/ARI/Silhouette), and geometric rank correlation (Spearman) against a geometry oracle. Full metric definitions and cross-type retrieval tables are in the Supplement.

Table 3 (left) shows that text encoders lead on within-type ranking (nDCG: E5 86.7 vs. SBM 68.2), while SBM maintains near-perfect triplet accuracy (99.9)

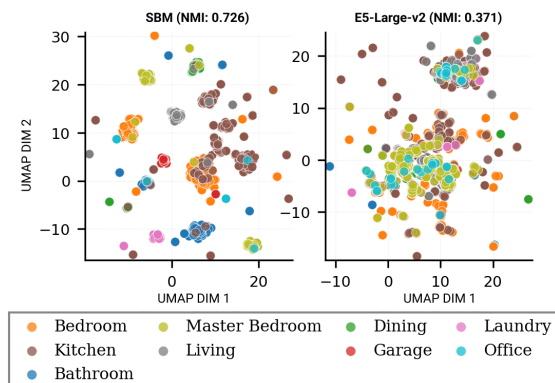


**Fig. 4:** UMAP visualization of room embeddings colored by room type. SBM (left, NMI: 0.726) produces well-separated clusters, while E5-Large-v2 (right, NMI: 0.371) shows intermingled boundaries. The nearly  $2\times$  higher NMI reflects SBM’s specialization in geometric and spatial structure over semantic similarity alone.

and comparable entity overlap (77.0). However, Table 3 (right) reveals that SBM yields substantially better global organization (NMI 0.726 vs. 0.335–0.371, ARI 0.437 vs.  $\leq 0$ ), demonstrating nearly twice the clustering quality (Fig. 4). This tighter type-structured embedding space—where rooms of the same category cluster more coherently—is a critical property for retrieval-augmented generation in architectural design.

## 5 Conclusion

We introduced SBM, a Transformer that encodes BIM room layouts as sparse attribute–feature matrices of mixed categorical and continuous tokens, supporting both encoder-only room embeddings and encoder–decoder generation (DDEP) within a single backbone. DDEP achieves near-complete inventory satisfaction, state-of-the-art navigability, and the lowest violation rates across LLM/VLM and domain-specific baselines; encoder-only embeddings yield substantially better within-type clustering than generic text encoders. A controlled same-data benchmark confirms that these gains are architectural, with ablations identifying joint continuous-feature embedding and entity ordering as the primary drivers. These results suggest that modestly sized, domain-specific sequence models over well-designed BIM tokenizations can outperform much larger general-purpose systems. Because DDEP outputs are BIM-native tokens, they can be consumed by downstream agentic systems for iterative LLM-driven refinement, opening a path toward human-in-the-loop layout co-design.

*Limitations.* Advanced vertical constraints like sloped ceilings or stairs/elevation changes, and MEP/service routing are not modeled. Our controlled baselines (ATISS, BLT) require representational bridges from their native formats to our BIM tokenization, which may not fully preserve their design strengths. The

benchmark comprises residential rooms from our corpus; existing public indoor-scene datasets (e.g., 3D-FRONT) use axis-aligned bounding boxes in global coordinates and lack the wall-referenced, parametric BIM entities our tokenization targets, precluding direct evaluation on those benchmarks. To enable reproducibility and follow-on work, we will release an anonymized dataset subset, evaluation suite, and code upon acceptance. Extending to non-residential typologies, diverse architectural styles, and varied local codes is left for future work.

## References

1. Carpo, M.: *The Alphabet and the Algorithm*. The MIT Press, 1st edn. (2011)
2. Carpo, M.: *The second digital turn: design beyond intelligence*. MIT press (2017)
3. Eastman, C.N.: *Spatial synthesis in computer-aided building design*. Elsevier Science Inc. (1975)
4. Eastman, C.N.: The Use of Computers Instead of Drawings in Building Design. *AIA Journal* **63** (Jan 1975)
5. Feng, W., Zhu, W., Fu, T.J., Jampani, V., Akula, A.R., He, X., Basu, S., Wang, X.E., Wang, W.Y.: Layoutgpt: Compositional visual planning and generation with large language models. In: *Advances in Neural Information Processing Systems* (2023), [https://proceedings.neurips.cc/paper\\_files/paper/2023/file/3a7f9e485845dac27423375c934cb4db-Paper-Conference.pdf](https://proceedings.neurips.cc/paper_files/paper/2023/file/3a7f9e485845dac27423375c934cb4db-Paper-Conference.pdf)
6. Flager, F., Haymaker, J.R.: A comparison of multidisciplinary design, analysis and optimization processes in the building construction and aerospace industries. In: *A comparison of multidisciplinary design, analysis and optimization processes in the building construction and aerospace industries* (2007), <https://api.semanticscholar.org/CorpusID:1539284>
7. Hu, R., Huang, Z., Tang, Y., van Kaick, O., Zhang, H., Huang, H.: Graph2plan: Learning floorplan generation from layout graphs. *arXiv preprint arXiv:2004.13204* (2020), <https://arxiv.org/abs/2004.13204>
8. Hu, S., et al.: MiDiffusion: Mixed diffusion for 3d indoor scene synthesis. *arXiv preprint arXiv:2405.21066* (2024), <https://arxiv.org/abs/2405.21066>
9. Kong, X., Jiang, L., Chang, H., Zhang, H., Hao, Y., Gong, H., Essa, I.: Blt: Bidirectional layout transformer for controllable layout generation. In: *Computer Vision – ECCV 2022: 17th European Conference, Tel Aviv, Israel, October 23–27, 2022, Proceedings, Part XVII*. p. 474–490. Springer-Verlag, Berlin, Heidelberg (2022). [https://doi.org/10.1007/978-3-031-19790-1\\_29](https://doi.org/10.1007/978-3-031-19790-1_29), [https://doi.org/10.1007/978-3-031-19790-1\\_29](https://doi.org/10.1007/978-3-031-19790-1_29)
10. Kán, P., Kaufmann, H.: Automated interior design using a genetic algorithm. In: *Proceedings of the 23rd ACM Symposium on Virtual Reality Software and Technology*. pp. 1–10. VRST '17, Association for Computing Machinery, New York, NY, USA (Nov 2017). <https://doi.org/10.1145/3139131.3139135>, <https://doi.org/10.1145/3139131.3139135>
11. Li, X., Sun, Y., Sha, Z.: Llm4cad: Multi-Modal large language models for three-dimensional computer-aided design generation. In: *Proceedings of the ASME 2024 International Design Engineering Technical Conferences and Computers and Information in Engineering Conference (IDETC/CIE 2024)*. vol. 88407, p. V006T06A015. ASME (2024), [https://sidilab.net/wp-content/uploads/2024/07/idetc2024\\_llm4cad\\_final.pdf](https://sidilab.net/wp-content/uploads/2024/07/idetc2024_llm4cad_final.pdf)

12. Li, Z., Zhang, X., Zhang, Y., Long, D., Xie, P., Zhang, M.: Towards general text embeddings with multi-stage contrastive learning. arXiv preprint arXiv:2308.03281 (2023)
13. Littlefair, G., Dutt, N.S., Mitra, N.J.: Flairgpt: Repurposing llms for interior designs (2025). <https://doi.org/10.48550/arXiv.2501.04648>, <https://arxiv.org/abs/2501.04648>, eUROGRAPHICS 2025
14. Liu, J., Xiong, W., Jones, I., Nie, Y., Gupta, A., Ouguz, B.: Clip-layout: Style-consistent indoor scene synthesis with semantic furniture embedding. ArXiv abs/**2303.03565** (2023), <https://api.semanticscholar.org/CorpusID:257378028>
15. Liu, Y., Wang, G.: Exploration of the Indoor Layout Optimization Model in Computer-Aided Visual Analysis. *Computer-Aided Design and Applications* pp. 167–180 (Aug 2024). <https://doi.org/10.14733/cadaps.2025.S4.167-180>, [https://cad-journal.net/files/vol\\_22/Vol22NoS4.html](https://cad-journal.net/files/vol_22/Vol22NoS4.html)
16. Merrell, P., Schkufza, E., Li, Z., Agrawala, M., Koltun, V.: Interactive furniture layout using interior design guidelines. *ACM Trans. Graph.* **30**(4), 87:1–87:10 (Jul 2011). <https://doi.org/10.1145/2010324.1964982>, <https://doi.org/10.1145/2010324.1964982>
17. Monedero, J.: Parametric design: a review and some experiences. *Automation in Construction* **9**(4), 369–377 (2000). [https://doi.org/https://doi.org/10.1016/S0926-5805\(99\)00020-5](https://doi.org/https://doi.org/10.1016/S0926-5805(99)00020-5), <https://www.sciencedirect.com/science/article/pii/S0926580599000205>
18. Nauata, N., Chang, W.C.M., Furukawa, Y., et al.: House-gan++: Generative adversarial layout refinement network towards intelligent computational agent. In: *CVPR (2021)*, [https://openaccess.thecvf.com/content/CVPR2021/html/Nauata\\_House-GAN\\_Generative\\_Adversarial\\_Layout\\_Refinement\\_Network\\_towards\\_Intelligent\\_Computational\\_Agent\\_CVPR\\_2021\\_paper.html](https://openaccess.thecvf.com/content/CVPR2021/html/Nauata_House-GAN_Generative_Adversarial_Layout_Refinement_Network_towards_Intelligent_Computational_Agent_CVPR_2021_paper.html)
19. Nguyen, H.T., Chen, Y., Voleti, V., Jampani, V., Jiang, H.: Housecrafter: Lifting floorplans to 3d scenes with 2d diffusion model. In: arXiv preprint arXiv:2406.20077 (2024), <https://arxiv.org/abs/2406.20077>
20. Paschalidou, D., Kar, A., Shugrina, M., Kreis, K., Geiger, A., Fidler, S.: Atiss: Autoregressive transformers for indoor scene synthesis. In: *Advances in Neural Information Processing Systems (NeurIPS) (2021)*
21. Ran, X., et al.: Directlayout: Direct numerical layout generation for 3d indoor scene synthesis. arXiv preprint arXiv:2506.05341 (2025), <https://arxiv.org/abs/2506.05341>
22. Shabani, M.A., Hosseini, S., Furukawa, Y.: Housediffusion: Vector floorplan generation via a diffusion model with discrete and continuous denoising (2022). <https://doi.org/10.48550/arXiv.2211.13287>, <https://arxiv.org/abs/2211.13287>
23. Song, P., Zheng, Y., Jia, J., Gao, Y.: Web3D-based automatic furniture layout system using recursive case-based reasoning and floor field. *Multimedia Tools and Applications* **78**(4), 5051–5079 (Feb 2019). <https://doi.org/10.1007/s11042-018-6334-5>, <https://doi.org/10.1007/s11042-018-6334-5>
24. Srivastava, D., et al.: Lay-your-scene: Natural scene layout generation with diffusion transformers. arXiv preprint arXiv:2505.04718 (2025), <https://arxiv.org/abs/2505.04718>
25. Sun, F.Y., Liu, W., Gu, S., Lim, D., Bhat, G., Tombari, F., Li, M., Haber, N., Wu, J.: Layoutvlm: Differentiable optimization of 3d layout via vision-language models. In: *Proceedings of the IEEE/CVF Conference on Computer Vision and Pattern Recognition (CVPR)*. pp. 29469–29478 (2025), <https://openaccess.thecvf.com/>

- content/CVPR2025/papers/Sun\_LayoutVLM\_Differentiable\_Optimization\_of\_3D\_Layout\_via\_Vision-Language\_Models\_CVPR\_2025\_paper.pdf
26. Sun, X., et al.: SemLayoutDiff: Semantic layout generation with diffusion models. arXiv preprint arXiv:2508.18597 (2025), <https://arxiv.org/abs/2508.18597>
  27. Tanasra, H., Rott Shaham, T., Michaeli, T., Austern, G., Barath, S.: Automation in Interior Space Planning: Utilizing Conditional Generative Adversarial Network Models to Create Furniture Layouts. *Buildings* **13**(7), 1793 (Jul 2023). <https://doi.org/10.3390/buildings13071793>, <https://www.mdpi.com/2075-5309/13/7/1793>, publisher: Multidisciplinary Digital Publishing Institute
  28. Wang, L., Yang, N., Huang, X., Jiao, B., Yang, L., Jiang, D., Majumder, R., Wei, F.: Text embeddings by weakly-supervised contrastive pre-training. arXiv preprint arXiv:2212.03533 (2022)
  29. Wang, X., Yeshwanth, C., Nießner, M.: Sceneformer: Indoor scene generation with transformers. arXiv preprint arXiv:2012.09793 (2020)
  30. Xiao, S., Liu, Z., Zhang, P., Muennighoff, N.: C-pack: Packaged resources to advance general chinese embedding (2023)
  31. Xu, K., Wu, L., Wang, Z., Feng, Y., Witbrock, M., Sheinin, V.: Graph2seq: Graph to sequence learning with attention-based neural networks (2018), <https://arxiv.org/abs/1804.00823>
  32. Yin, J., Zeng, P., Zhong, J., Li, P., Zhang, M., Luo, R., Lu, S.: Floorplan-deepseek (fpds): A multimodal approach to floorplan generation using vector-based next room prediction. arXiv preprint **arXiv:2506.21562** (2025), <https://arxiv.org/pdf/2506.21562>
  33. Zong, Z., Chen, G., Zhan, Z., Yu, F., Tan, G.: Housetune: Two-stage floorplan generation with LLM assistance (2024). <https://doi.org/10.48550/arXiv.2411.12279>, <https://arxiv.org/abs/2411.12279>